HHS Public Access

Author manuscript

Nat Chem. Author manuscript; available in PMC 2014 July 01.

Published in final edited form as:

Nat Chem. 2014 January ; 6(1): 28–33. doi:10.1038/nchem.1795.

Oligomerization transforms human APOBEC3G from an efficient enzyme to a slowly dissociating nucleic acid binding protein

Kathy R. Chaurasiya[1], **Micah J. McCauley**[1], **Wei Wang**[2], **Dominic F. Qualley**[2], **Tiyun Wu**[3], **Shingo Kitamura**[4], **Hylkje Geertsema**[1], **Denise S.B. Chan**[5], **Amber Hertz**[3], **Yasumasa Iwatani**[3,4], **Judith G. Levin**[3], **Karin Musier-Forsyth**[2], **Ioulia Rouzina**[6], and **Mark C. Williams**[1,*]

[1]Department of Physics, Northeastern University, Boston, MA 02115

[2]Department of Chemistry and Biochemistry, Center for Retrovirus Research, and Center for RNA Biology, The Ohio State University, Columbus, OH 43210

[3]Section on Viral Gene Regulation, Program on Genomics of Differentiation, Eunice Kennedy Shriver National Institute of Child Health and Human Development, National Institutes of Health, Bethesda, MD 20892

[4]Clinical Research Center, National Hospital Organization Nagoya Medical Center, Nagoya, Aichi 460-0001, Japan

[5]Department of Structural Biology, University of Pittsburgh School of Medicine, Pittsburgh, PA 15260

[6]Department of Biochemistry, Molecular Biology and Biophysics, University of Minnesota, Minneapolis, MN 55455

Abstract

The human APOBEC3 proteins are a family of DNA-editing enzymes that play an important role in the innate immune response and have broad activity against retroviruses and retrotransposons. APOBEC3G is a member of this family that inhibits HIV-1 replication in the absence of the viral infectivity factor Vif. Inhibition of HIV replication occurs by both deamination of viral single-stranded DNA and a deamination-independent mechanism. Efficient deamination requires rapid binding to and dissociation from ssDNA. However, a relatively slow dissociation rate is required for the proposed deaminase-independent roadblock mechanism in which APOBEC3G binds the viral template strand and blocks reverse transcriptase-catalyzed DNA elongation. Here we show that APOBEC3G initially binds ssDNA with rapid on-off rates and subsequently converts to a slowly dissociating mode. In contrast, an oligomerization-deficient APOBEC3G mutant did not exhibit a slow off rate. We propose that catalytically active monomers or dimers slowly oligomerize on the viral genome and inhibit reverse transcription.

*Correspondence should be addressed to: MCW. mark@neu.edu.

AUTHOR CONTRIBUTIONS

MCW, KRC, and IR designed experiments; KRC performed experiments and analyzed data; MM performed experiments with the mutant; HG performed preliminary experiments; SK, WW, DFQ, TW, YI, DC, and AH prepared the proteins; IR developed the binding model; KRC, MCW, IR, JGL, and KMF wrote the manuscript.

Keywords

APOBEC; DNA binding; HIV-1; restriction factor; roadblock mechanism; optical tweezers; single molecule force spectroscopy

TEXT

APOBEC3 proteins are DNA-editing enzymes that are part of the innate human immune response to viral pathogens, including retroviruses and retrotransposons[1–4]. Of all the A3 proteins, A3G[5] is the most potent inhibitor of HIV-1 replication[1,4,6], reducing viral infectivity by several orders of magnitude in the absence of the HIV-1 viral infectivity factor Vif[7–9]. In fact, the function of Vif is to specifically counteract the antiviral activity of A3G[1,9].

Although A3G is the most studied of all the APOBEC proteins, the molecular mechanism for A3G-mediated HIV-1 restriction is still not fully understood. A3G is a deoxycytidine deaminase, which converts deoxycytidine bases in single-stranded DNA (ssDNA) to deoxyuridine[5,10–14]. A3G deamination of minus-strand viral DNA formed during reverse transcription results in G to A hypermutation in the plus-strand[11,12,15], which effectively impairs viral replication. However, there are several lines of evidence that suggest that a deaminase-independent mechanism is also involved[1,6,20]. First, A3G catalytic mutants retain antiviral activity[16–19]. Second, A3G inhibits hepatitis B virus replication without G to A hypermutation[21]. Third, A3A inhibits LINE-1 and Alu retrotransposition[22–28] and parvovirus replication[24,29] independent of deaminase activity. Further evidence for a non-editing mechanism is based on the reduction of minus-strand viral DNA levels in HIV-1 particles during endogenous reverse transcription[30], inhibition of reverse transcriptase (RT)-catalyzed viral DNA elongation *in vitro* by catalytic A3G mutants[31,32], inhibition of strand transfer reactions *in vitro* and in cell-based assays[32–34], and A3G-induced inhibition of reverse transcription in viruses from human $CD4^+$ T cells[35]. A roadblock model, in which A3G molecules bind the template strand at one or a few locations and physically block viral DNA synthesis, has therefore been proposed as a molecular mechanism for deaminase-independent inhibition[32].

Since only 7 (± 4) A3G molecules are incorporated into each *vif*-deficient virion[36], RT inhibition by an A3G roadblock requires a slow A3G off-rate from single-stranded nucleic acids. In contrast, these few A3G molecules must have fast on-off rates to deaminate up to 1000 sites in several minutes[14] using a rapid search mechanism on viral ssDNA[37,38]. To resolve this apparent paradox, we hypothesize that A3G exhibits fast binding kinetics as a monomer or dimer in order to function as an efficient enzyme, and slow kinetics upon oligomerization in order to block RT from elongating viral DNA. To test this idea, we used optical tweezers to monitor A3G binding kinetics on a single DNA molecule.

RESULTS

Single molecule measurements of A3G binding to ssDNA

For these studies, a single double-stranded λ-DNA molecule was tethered to two polystyrene beads, with one bead held in an optical trap and another on a micropipette tip. As the fixed bead is gradually moved away from the optically-trapped bead, the force on the DNA molecule is measured at each extension, yielding a force-extension curve (Fig. 1, solid black line). The solution surrounding the single DNA molecule can be exchanged in order to measure the effects of DNA binding ligands on the properties of DNA.

In the absence of binding ligands, force-induced melting occurs at a constant force of 61.0 ± 0.5 pN, generating ssDNA, either by peeling from the ends or forming melting bubbles[39]. Although a stretched form of dsDNA called S-DNA may form upon overstretching at high salt, it is well-established that overstretching is force-induced melting in the presence of ssDNA binding proteins and at the ionic strength used in this work[39,40]. At the end of the overstretching transition, the bead movement reverses direction and DNA tension is gradually released (Fig. 1, dashed black line). The minimal hysteresis, or mismatch between DNA extension and release, indicates that the ssDNA generated by force reanneals immediately into dsDNA during the return. At any given point along the transition, the molecule is a well-characterized combination of dsDNA and ssDNA (Supplementary Eq. S3)[40]. Pausing at fixed extension during the melting transition allows precise control of the fraction of ssDNA substrate available for protein binding.

The force-extension curve probes the length of the captured DNA molecule at a given force. At forces above 7 pN, ssDNA is longer than dsDNA. We exploit this force-dependent difference in length to measure the ssDNA binding properties of A3G. A3G-saturated ssDNA, obtained at high protein concentration by first overstretching DNA and allowing A3G to fully bind and stabilize the DNA in its single-stranded form, is longer than dsDNA and shorter than ssDNA (Fig. 1). Therefore, A3G bound to ssDNA increases the molecule in length by Δx_b below the melting transition, and decreases the length by Δx_a above the melting transition.

In the presence of 50 nM A3G, the extension curve follows the DNA-only curve before the melting transition, reflecting no measurable binding to dsDNA (Fig. 2, panel **a**, solid line). A3G only binds after force-induced melting generates ssDNA. Based on the observed hysteresis (Fig. 2, panel **a**, dashed line), most of the protein does not dissociate upon DNA release and prevents the two strands from fully reannealing. A3G-bound ssDNA is longer than dsDNA (Fig. 1), so the change in length at a given force (Fig. 2, panel **a**, Δx_t) describes the total fraction of A3G bound to ssDNA (f_{total}, see Supplementary Fig. 1, panel **a** online).

A second stretch of the same molecule does not retrace the release curve, revealing that some fraction of the protein has dissociated during the 30 s incubation at zero force between stretch-release cycles (Fig. 2, panel **b**). As soon as any A3G dissociates at forces below the force-induced melting transition, the two strands reanneal into dsDNA, which is shorter than A3G-bound ssDNA (Fig. 2, panel **b**, Δx_f). Therefore the second stretch reflects the fraction of A3G that remains ssDNA-bound (f_{slow}), which allows the fraction that dissociates quickly

(f_{fast}) to be quantified as $f_{fast} = f_{total} - f_{slow}$. The DNA was held at zero force between the first release and the second stretch for 30 s, but longer wait times up to 120 minutes do not lead to further measurable dissociation (data not shown for clarity).

A3G was exposed to ssDNA for 50 s in this experiment. However, A3G oligomerization observed in bulk experiments occurs on much longer timescales[37]. To measure slow binding, A3G was incubated for 250 s with ssDNA generated by force-induced melting (Fig. 2, panel **c**). The DNA release curve obtained after this incubation exhibits a length increase relative to the initial release curve (Fig. 2, panel **c**, Δx_i) because additional A3G binds ssDNA during incubation. This effect increases at longer incubation times (Fig. 2, panel **d**), approaching the A3G-saturated ssDNA curve (shown in Fig. 1).[41] Fits to the DNA release curves at increasing incubation time yield $f_{total}(t)$, while the subsequent stretch (data not shown for clarity) quantifies $f_{slow}(t)$, and $f_{fast}(t)$ is the difference between the two. These measurements for 50 nM A3G are presented in Fig. 3, panel **a**.

Quantitative binding model

The slow binding component increases at the expense of the fast component, suggesting that the A3G-ssDNA reaction may be modeled as a two-step process:

$$A3G + ssDNA \underset{k_{-1}}{\overset{k_1 c}{\rightleftharpoons}} (A3G/ssDNA)_{fast} \underset{k_{-2}}{\overset{k_2}{\rightleftharpoons}} (A3G/ssDNA)_{slow}, \quad 1$$

in which an initial bimolecular process leads to a fast complex that converts to a slow, more stable complex in the second unimolecular step. Binding rates were obtained from fits to this model (Supplementary Eqs. S9–S11) at five A3G concentrations (Fig. 3, panel **b**). (A3G precipitates at high concentrations[18], so experiments were calibrated using force-extension curves at known protein concentrations.) As expected, the observed fast rate k_{fast} and the on rate $k_1 c$ are both linear with A3G concentration (Fig. 3, panel **c**). The bimolecular rate constant $k_1 = 1.5\ (\pm\ 0.1) \times 10^5\ M^{-1}s^{-1}$ and off rate $k_{-1} = 1.2\ (\pm\ 0.1) \times 10^{-2}\ s^{-1}$ are consistent with single molecule FRET[42] and fluorescence spectroscopy[37] measurements, considering differences in solution conditions. The observed slow rate k_{slow} saturates at high A3G concentration (Fig. 3, panel **d**), and both the on and off rates for the second, unimolecular step are concentration-independent ($k_2 = 6.7\ (\pm\ 0.6) \times 10^{-3}\ s^{-1}$ and $k_{-2} = 2.8\ (\pm\ 0.5) \times 10^{-5}\ s^{-1}$). Elementary reaction rates were obtained from the data in several different ways, and agreement of the resulting values (see Supplementary Table 2 online) supports the binding model.

Oligomerization is responsible for slow binding

To determine whether slow binding is due to A3G oligomerization, we expressed and purified the F126A/W127A A3G mutant (A3G FW), which is severely defective in oligomerization[41]. When this mutant was incubated with ssDNA for 1050 s, the release curve exhibited minimal hysteresis (Fig. 4, panel **a**), and all the bound protein dissociated prior to the subsequent stretch (Fig. 4, panel **b**). A direct comparison of the hysteresis observed for both wild type and mutant A3G is shown in Fig. 4, panel **c**. The lack of a slow ssDNA bound fraction observed for the mutant, along with the striking difference between

the hysteresis observed for the two proteins, shows that the oligomerization-defective mutant does not exhibit slow ssDNA binding kinetics. Thus, we conclude that the slow kinetics observed for wild type A3G is due to oligomerization.

DISCUSSION

Here we use a single molecule method that allows us to quantify two distinct modes of A3G binding to ssDNA and characterize the conversion of a fast state into a slow state. These results suggest a binding mechanism in which monomers or dimers initially bind ssDNA and rapidly reach equilibrium ($1/k_{fast}$ = 24 ± 1 s at 200 nM), before slowly converting to oligomers ($1/k_{slow}$ = 206 ± 20 s) (Fig. 5, panel **a**). Previous bulk solution experiments have established that A3G oligomerizes in the presence of single-stranded nucleic acids[41,43], which inhibits efficient deaminase activity[41]. We also demonstrate that an A3G mutant (F126A/W127A) that is severely compromised in oligomerization, but retains deaminase activity, does not exhibit slow binding kinetics. Furthermore, a recent study shows that a similar oligomerization-defective mutant (W127A) inhibits deamination-independent viral restriction[44]. These observations support the hypothesis that A3G oligomerization is responsible for deaminase-independent inhibition of viral replication.

In light of these quantitative results *in vitro*, we propose a model for A3G's effects on HIV-1 replication. A3G oligomerizes on viral RNA when it is packaged inside the virion[43,45], stalling RT during minus-strand synthesis. RT pauses until the oligomer dissociates, or switches to the other RNA template strand, circumventing the A3G roadblock and leading to partial inhibition of reverse transcription[35]. In contrast to our *in vitro* studies, the maximum size of the A3G oligomer may be limited by the small number of A3G molecules packaged in virions[36]. These limitations on oligomer size may lead to higher off rates *in virio*. Once the A3G oligomer dissociates during minus-strand synthesis, the monomers or dimers that are released have low affinity for the newly formed RNA-DNA duplex[14,18]. As RNase H activity exposes the minus strand, all A3G molecules bind the ssDNA template within a second, as indicated by $1/k_1$ = 0.7 ± 0.1 s when fast binding rates are extrapolated to the estimated 13 ± 8 μM A3G concentration in the virion[32]. A3G remains bound in a rapid sliding mode[37,42] for $1/k_{-1}$ = 85 ± 5 s, which allows high deamination rates[37,38] until oligomerization forms a roadblock to plus-strand synthesis after $1/k_2$ = 149 ± 13 s (Fig. 5, panel **b**).

The *in virio* model that we propose based on our measurements is consistent with the available data on A3G function. Recent cell-based experiments demonstrate that A3G uniformly blocks minus-strand synthesis in the absence of preferred RT termination sites along the viral template[35]. However, this does not necessarily indicate that A3G binds throughout the length of the genomic RNA. Oligomerization is nucleic acid sequence-independent and therefore we expect the roadblock to form at a small number of random sites along the viral genome, as observed *in virio*. Although A3G may bind RT in an RNA-independent interaction[46], a recent report concludes that there is no direct interaction between A3G and RT[31]. In any case, this type of binding is equally probable for any of the 100 RT heterodimers present in the virion[47] and the probability that one of 7 ± 4 A3G molecules binds and inhibits the catalytically active RT molecule is therefore less than 10%.

Thus, a possible A3G-RT interaction appears unlikely to be primarily responsible for A3G-induced inhibition of reverse transcription.

The data we present resolve seemingly contradictory mechanisms for A3G inhibition of viral replication by demonstrating that A3G can function as both a fast deaminase and a slow nucleic acid binding protein. Regulation of enzymatic activity via protein oligomerization may be a general property of other APOBEC family members that inhibit replication of retroviruses and retrotransposons independent of deaminase activity. The single molecule method described here does not require labeling of DNA or protein and is optimal for measuring the biologically important process of slow protein oligomerization on ssDNA.

METHODS

A3G preparation and purification

Recombinant WT A3G and A3G FW were expressed in a baculovirus expression system using an N-terminal glutathione S-transferase (GST) tag and purified. The GST tag was then removed using a Novagen Enterokinase Cleavage Capture Kit. The deaminase activity of purified wild type A3G was verified using a gel-based uracil DNA glycosylase assay after removal of the GST tag. A similar method was used to verify the enzymatic activity of purified GST-tagged A3G FW. Additional protein preparation details are supplied in the Supplementary Methods.

Single molecule experiments

Biotin-labeled bacteriophage λ DNA was captured between two streptavidin-coated polystyrene beads, one on a fixed micropipette tip and the other held in an optical trap, as described in Supplementary Methods. The DNA was extended by moving the micropipette tip at a rate of 100 nm/s, and the resulting force on the bead in the trap was recorded in order to obtain the force-extension curve for DNA alone. The buffer surrounding the DNA molecule was then exchanged for a solution of fixed protein concentration. Force-extension curves in the presence and absence of protein were fit to the Worm-Like Chain model for dsDNA (Supplementary Eq. S1) and the Freely-Jointed Chain model (Supplementary Eq. S2) for ssDNA. The A3G-saturated ssDNA force-extension curve was fit to Supplementary Eq. S4. Measurements of the fraction of ssDNA bound by protein were then determined by fitting force-extension curves to the linear combination of dsDNA extension and A3G-bound ssDNA extension, as shown in Supplementary Eqs S6 and S7.

Two-step binding model

The kinetics of protein-DNA binding was fit to a two-step binding model, in which it was assumed that an initial fast bimolecular binding event was followed by a slow unimolecular binding event, as described by Supplementary Eqs. S9–S11, yielding measured fast and slow binding rates k_{fast} and k_{slow}. By then fitting the concentration-dependent measurements of k_{fast} and k_{slow} to the reaction shown in Eq. 1, we determine the elementary reaction rates for each step k_1, k_{-1}, k_2, and k_{-2}, as well as the elementary equilibrium constants for each step K_1 and K_2, as described in Supplementary Methods.

Supplementary Material

Refer to Web version on PubMed Central for supplementary material.

Acknowledgments

The authors thank Darja Pollpeter, Michael H. Malim, and David Rueda for valuable discussions, and Myron F. Goodman for his generous gift of the F126A/W127A mutant clone. This work was supported in part by NIH [GM072462] and NSF [MCB-1243883] (MCW), NIH [GM065056] (KMF), and the NIH Intramural Research Program (NICHD) (JGL). KRC was supported by the NSF IGERT Program [DGE-0504331].

References

1. Malim MH. APOBEC proteins and intrinsic resistance to HIV-1 infection. Philos Trans R Soc Lond B Biol Sci. 2009; 364(1517):675–687. [PubMed: 19038776]
2. Harris RS, Liddament MT. Retroviral restriction by APOBEC proteins. Nat Rev Immunol. 2004; 4(11):868–877. [PubMed: 15516966]
3. Duggal NK, Emerman M. Evolutionary conflicts between viruses and restriction factors shape immunity. Nat Rev Immunol. 2012; 12(10):687–695. [PubMed: 22976433]
4. Chiu YL, Greene WC. The APOBEC3 cytidine deaminases: An innate defensive network opposing exogenous retroviruses and endogenous retroelements. Annu Rev Immunol. 2008; 26:317–353. [PubMed: 18304004]
5. Sheehy AM, Gaddis NC, Choi JD, Malim MH. Isolation of a human gene that inhibits HIV-1 infection and is suppressed by the viral Vif protein. Nature. 2002; 418(6898):646–650. [PubMed: 12167863]
6. Holmes RK, Malim MH, Bishop KN. APOBEC-mediated viral restriction: not simply editing? Trends Biochem Sci. 2007; 32(3):118–128. [PubMed: 17303427]
7. Fisher AG, Ensoli B, Ivanoff L, Chamberlain M, Petteway S, Ratner L, et al. The sor gene of HIV-1 is required for efficient virus transmission in vitro. Science. 1987; 237(4817):888–893. [PubMed: 3497453]
8. Strebel K, Daugherty D, Clouse K, Cohen D, Folks T, Martin MA. The HIV 'A' (sor) gene product is essential for virus infectivity. Nature. 1987; 328(6132):728–730. [PubMed: 2441266]
9. Goila-Gaur R, Strebel K. HIV-1 Vif, APOBEC, and intrinsic immunity. Retrovirology. 2008; 5(1): 1–16. [PubMed: 18177500]
10. Lecossier D, Bouchonnet F, Clavel F, Hance AJ. Hypermutation of HIV-1 DNA in the absence of the Vif protein. Science. 2003; 300(5622):1112. [PubMed: 12750511]
11. Mangeat B, Turelli P, Caron G, Friedli M, Perrin L, Trono D. Broad antiretroviral defence by human APOBEC3G through lethal editing of nascent reverse transcripts. Nature. 2003; 424(6944): 99–103. [PubMed: 12808466]
12. Zhang H, Yang B, Pomerantz RJ, Zhang CM, Arunachalam SC, Gao L. The cytidine deaminase CEM15 induces hypermutation in newly synthesized HIV-1 DNA. Nature. 2003; 424(6944):94–98. [PubMed: 12808465]
13. Suspène R, Sommer P, Henry M, Ferris S, Guetard D, Pochet S, et al. APOBEC3G is a single-stranded DNA cytidine deaminase and functions independently of HIV reverse transcriptase. Nucleic Acids Res. 2004; 32(8):2421–2429. [PubMed: 15121899]
14. Yu Q, Konig R, Pillai S, Chiles K, Kearney M, Palmer S, et al. Single-strand specificity of APOBEC3G accounts for minus-strand deamination of the HIV genome. Nat Struct Mol Biol. 2004; 11(5):435–442. [PubMed: 15098018]
15. Harris RS, Bishop KN, Sheehy AM, Craig HM, Petersen-Mahrt SK, Watt IN, et al. DNA deamination mediates innate immunity to retroviral infection. Cell. 2004; 116(4)
16. Newman ENC, Holmes RK, Craig HM, Klein KC, Lingappa JR, Malim MH, et al. Antiviral function of APOBEC3G can be dissociated from cytidine deaminase activity. Curr Biol. 2005; 15(2):166–170. [PubMed: 15668174]

17. Holmes RK, Koning FA, Bishop KN, Malim MH. APOBEC3F can inhibit the accumulation of HIV-1 reverse transcription products in the absence of hypermutation - Comparisons with APOBEC3G. J Biol Chem. 2007; 282(4):2587–2595. [PubMed: 17121840]
18. Iwatani Y, Takeuchi H, Strebel K, Levin JG. Biochemical activities of highly purified, catalytically active human APOBEC3G: Correlation with antiviral effect. J Virol. 2006; 80(12):5992–6002. [PubMed: 16731938]
19. Luo K, Wang T, Liu BD, Tian CJ, Xiao ZX, Kappes J, et al. Cytidine deaminases APOBEC3G and APOBEC3F interact with human immunodeficiency virus type 1 integrase and inhibit proviral DNA formation. J Virol. 2007; 81(13):7238–7248. [PubMed: 17428847]
20. Levin JG, Mitra M, Mascarenhas A, Musier-Forsyth K. Role of HIV-1 nucleocapsid protein in HIV-1 reverse transcription. RNA Biol. 2010; 7(6):754–774. [PubMed: 21160280]
21. Turelli P, Mangeat B, Jost S, Vianin S, Trono D. Inhibition of hepatitis B virus replication by APOBEC3G. Science. 2004; 303(5665):1829–1829. [PubMed: 15031497]
22. Bogerd HP, Wiegand HL, Doehle BP, Lueders KK, Cullen BR. APOBEC3A and APOBEC3B are potent inhibitors of LTR-retrotransposon function in human cells. Nucleic Acids Res. 2006; 34(1): 89–95. [PubMed: 16407327]
23. Bogerd HP, Wiegand HL, Hulme AE, Garcia-Perez JL, O'Shea KS, Moran JV, et al. Cellular inhibitors of long interspersed element 1 and Alu retrotransposition. P Natl Acad Sci USA. 2006; 103(23):8780–8785.
24. Chen H, Lilley CE, Yu Q, Lee DV, Chou J, Narvaiza I, et al. APOBEC3A is a potent inhibitor of adeno-associated virus and retrotransposons. Curr Biol. 2006; 16(5):480–485. [PubMed: 16527742]
25. Muckenfuss H, Hamdorf M, Held U, Perkovic M, Lower J, Cichutek K, et al. APOBEC3 proteins inhibit human LINE-1 retrotransposition. J Biol Chem. 2006; 281(31):22161–22172. [PubMed: 16735504]
26. Kinomoto M, Kanno T, Shimura M, Ishizaka Y, Kojima A, Kurata T, et al. All APOBEC3 family proteins differentially inhibit LINE-1 retrotransposition. Nucleic Acids Res. 2007; 35(9):2955–2964. [PubMed: 17439959]
27. Niewiadomska AM, Tian C, Tan L, Wang T, Sarkis PTN, Yu X-F. Differential inhibition of Long Interspersed Element 1 by APOBEC3 does not correlate with high-molecular-mass-complex formation or P-body association. J Virol. 2007; 81(17):9577–9583. [PubMed: 17582006]
28. Bulliard Y, Narvaiza I, Bertero A, Peddi S, Röhrig UF, Ortiz M, et al. Structure-function analyses point to a polynucleotide-accommodating groove essential for APOBEC3A restriction activities. J Virol. 2011; 85(4):1765–1776. [PubMed: 21123384]
29. Narvaiza I, Linfesty DC, Greener BN, Hakata Y, Pintel DJ, Logue E, et al. Deaminase-independent inhibition of parvoviruses by the APOBEC3A cytidine deaminase. PLoS Pathog. 2009 May.(5)
30. Bishop KN, Verma M, Kim EY, Wolinsky SM, Malim MH. APOBEC3G inhibits elongation of HIV-1 reverse transcripts. PLoS Pathog. 2008; 4(12)
31. Adolph MB, Webb J, Chelico L. Retroviral restriction factor APOBEC3G delays the initiation of DNA synthesis by HIV-1 reverse transcriptase. Plos One. 2013; 8(5):e64196. [PubMed: 23717565]
32. Iwatani Y, Chan DSB, Wang F, Maynard KS, Sugiura W, Gronenborn AM, et al. Deaminase-independent inhibition of HIV-1 reverse transcription by APOBEC3G. Nucleic Acids Res. 2007; 35(21):7096–7108. [PubMed: 17942420]
33. Li XY, Guo F, Zhang L, Kleiman L, Cen S. APOBEC3G inhibits DNA strand transfer during HIV-1 reverse transcription. J Biol Chem. 2007; 282(44):32065–32074. [PubMed: 17855362]
34. Mbisa JL, Barr R, Thomas JA, Vandegraaff N, Dorweiler IJ, Svarovskaia ES, et al. Human immunodeficiency virus type 1 cDNAs produced in the presence of APOBEC3G exhibit defects in plus-strand DNA transfer and integration. J Virol. 2007; 81(13):7099–7110. [PubMed: 17428871]
35. Gillick K, Pollpeter D, Phalora P, Kim EY, Wolinsky SM, Malim MH. Suppression of HIV-1 infection by APOBEC3 proteins in primary human CD4+ T cells Is associated with inhibition of processive reverse transcription as well as excessive cytidine deamination. J Virol. 2013; 87(3): 1508–1517. [PubMed: 23152537]

36. Xu HZ, Chertova E, Chen JB, Ott DE, Roser JD, Hu WS, et al. Stoichiometry of the antiviral protein APOBEC3G in HIV-1 virions. Virology. 2007; 360(2):247–256. [PubMed: 17126871]
37. Chelico L, Sacho EJ, Erie DA, Goodman MF. A model for oligomeric regulation of APOBEC3G cytosine deaminase-dependent restriction of HIV. J Biol Chem. 2008; 283(20):13780–13791. [PubMed: 18362149]
38. Nowarski R, Britan-Rosich E, Shiloach T, Kotler M. Hypermutation by intersegmental transfer of APOBEC3G cytidine deaminase. Nat Struct Mol Biol. 2008; 15(10):1059–1066. [PubMed: 18820687]
39. King GA, Gross P, Bockelmann U, Modesti M, Wuite GJL, Peterman EJG. Revealing the competition between peeled ssDNA, melting bubbles, and S-DNA during DNA overstretching using fluorescence microscopy. P Natl Acad Sci USA. 2013
40. Chaurasiya KR, Paramanathan T, McCauley MJ, Williams MC. Biophysical characterization of DNA binding from single molecule force measurements. Phys Life Rev. 2010; 7(3):299–341. [PubMed: 20576476]
41. Chelico L, Prochnow C, Erie DA, Chen XS, Goodman MF. Structural model for deoxycytidine deamination mechanisms of the HIV-1 inactivation enzyme APOBEC3G. J Biol Chem. 2010; 285(21):16195–16205. [PubMed: 20212048]
42. Senavirathne G, Jaszczur M, Auerbach PA, Upton TG, Chelico L, Goodman MF, et al. Single-stranded DNA scanning and deamination by APOBEC3G cytidine deaminase at single molecule resolution. J Biol Chem. 2012; 287(19):15826–15835. [PubMed: 22362763]
43. Huthoff H, Autore F, Gallois-Montbrun S, Fraternali F, Malim MH. RNA-dependent oligomerization of APOBEC3G is required for restriction of HIV-1. PLoS Pathog. 2009; 5(3):e1000330. [PubMed: 19266078]
44. Bélanger K, Savoie M, Rosales Gerpe MC, Couture J-F, Langlois M-A. Binding of RNA by APOBEC3G controls deamination-independent restriction of retroviruses. Nucleic Acids Res. in press.
45. Soros V, Greene W. APOBEC3G and HIV-1: Strike and counterstrike. Current HIV/AIDS Reports. 2007; 4(1):3–9. [PubMed: 17338854]
46. Wang XX, Ao ZJ, Chen LY, Kobinger G, Peng JY, Yao XJ. The cellular antiviral protein APOBEC3G interacts with HIV-1 reverse transcriptase and inhibits its function during viral replication. J Virol. 2012; 86(7):3777–3786. [PubMed: 22301159]
47. Coffin, JM.; Hughes, SH.; Varmus, HE. Retroviruses. Cold Spring Harbor Laboratory Press; Cold Spring Harbor NY: 1997.
48. Vo MN, Barany G, Rouzina I, Musier-Forsyth K. Mechanistic studies of mini-TAR RNA/DNA annealing in the absence and presence of HIV-1 nucleocapsid protein. J Mol Biol. 2006; 363(1): 244–261. [PubMed: 16962137]

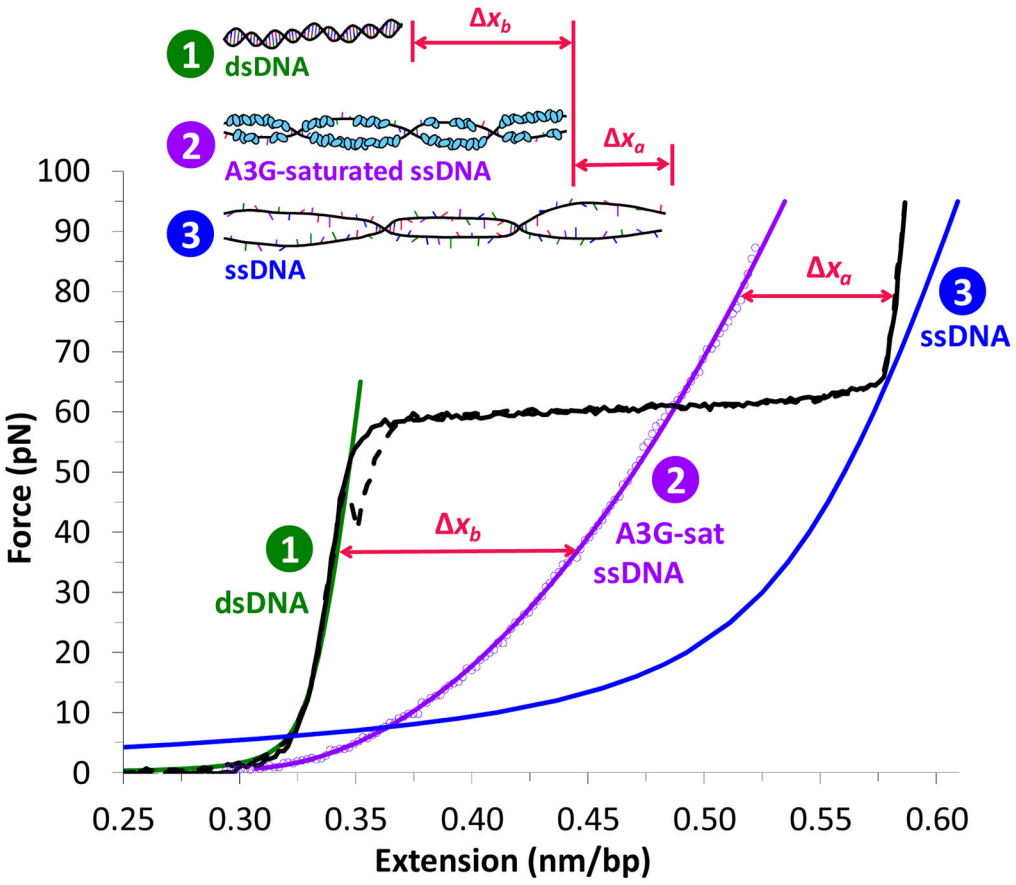

Figure 1.

The force-dependent difference in length between DNA and a saturated A3G-DNA complex allows us to measure A3G binding. Typical extension (solid black) and return (dashed black) of a single DNA molecule. At 61.0 ± 0.5 pN, the molecule undergoes a force-induced melting transition from dsDNA (green, Eq. S1) to ssDNA (blue). A3G-saturated ssDNA (200 nM A3G, $t > 500$ s, data points fit to Eq. S4, solid purple) is longer than dsDNA (Δx_b below the melting transition) and shorter than ssDNA (Δx_a above the melting transition). A3G-saturated ssDNA is significantly shorter than ssDNA only (blue, Eq. S2), which suggests that A3G may wrap ssDNA upon binding.

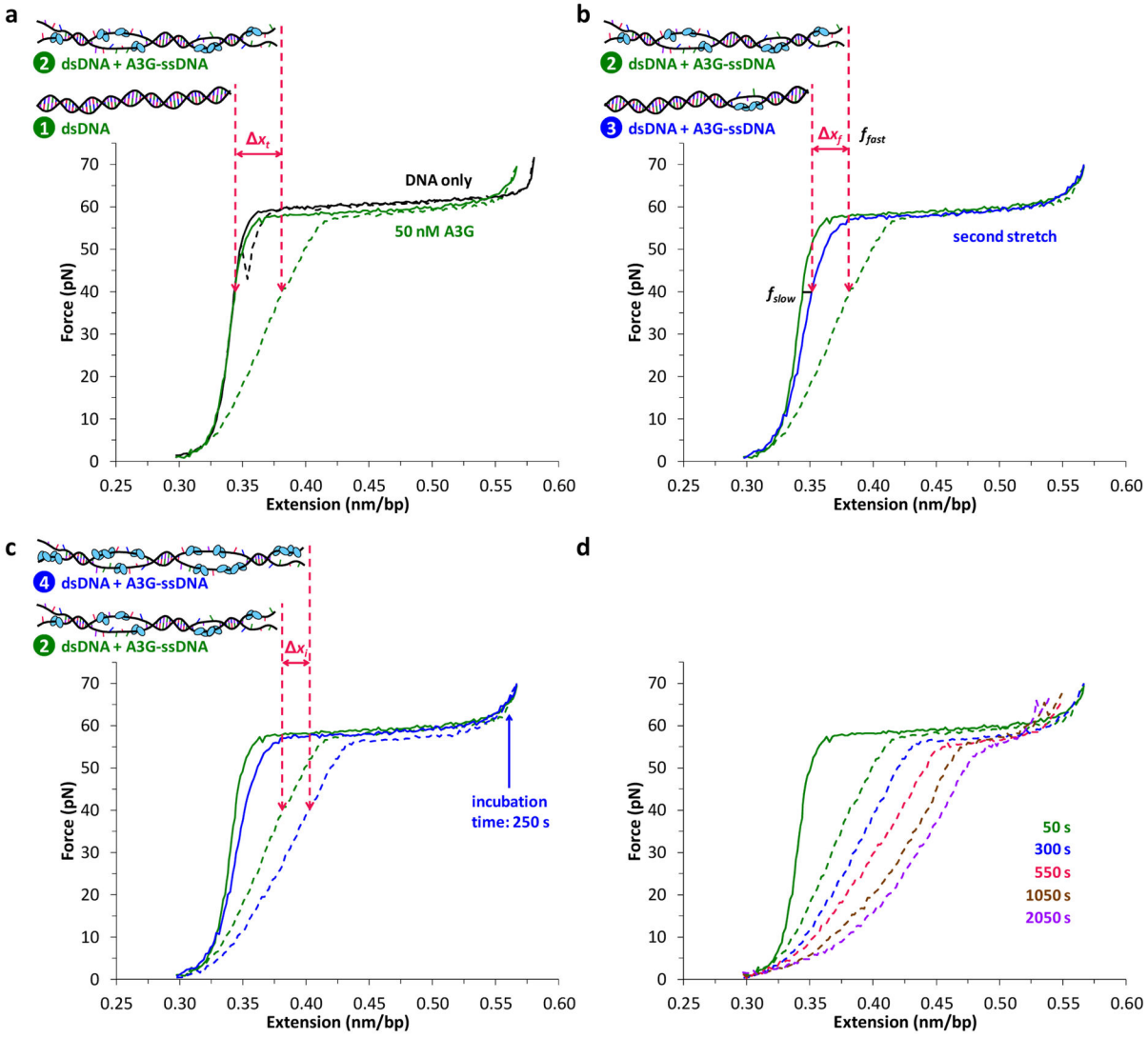

Figure 2.

Single molecule method to measure fast and slow fractions of A3G binding. (**A**) Without protein (black), a single DNA molecule reanneals immediately upon release, exhibiting minimal hysteresis, or mismatch between stretch (solid) and release (dashed) curves. In the presence of 50 nM A3G, the stretch curve (solid green) follows the dsDNA-only curve, indicating negligible A3G-dsDNA binding. A3G binds the exposed ssDNA, and prohibits the DNA strands from reannealing, resulting in hysteresis (dashed green). For a given force (40 pN shown), there is a corresponding change in DNA length Δx_t between A3G-free dsDNA (left arrow, drawing 1) and partially A3G-bound ssDNA (right arrow, drawing 2). This force-dependent length change measures A3G-ssDNA binding (Supplementary Fig. 1). (**B**) The second stretch (solid blue) lies between the first stretch and release curves, distinguishing the fraction of A3G that remains bound (f_{slow}) from the fraction that dissociated (f_{fast}) before the second stretch. The A3G that dissociates rapidly allows the strands to reanneal immediately into dsDNA (drawing 3), resulting in length decrease Δx_f. (**C**) Pausing at fixed DNA extension after incubating ssDNA with 50 nM A3G results in

additional binding (drawing 4), indicated by the corresponding length increase Δx_i measured during DNA release. (**D**) A3G binding increases with total exposure time to ssDNA (dashed lines).

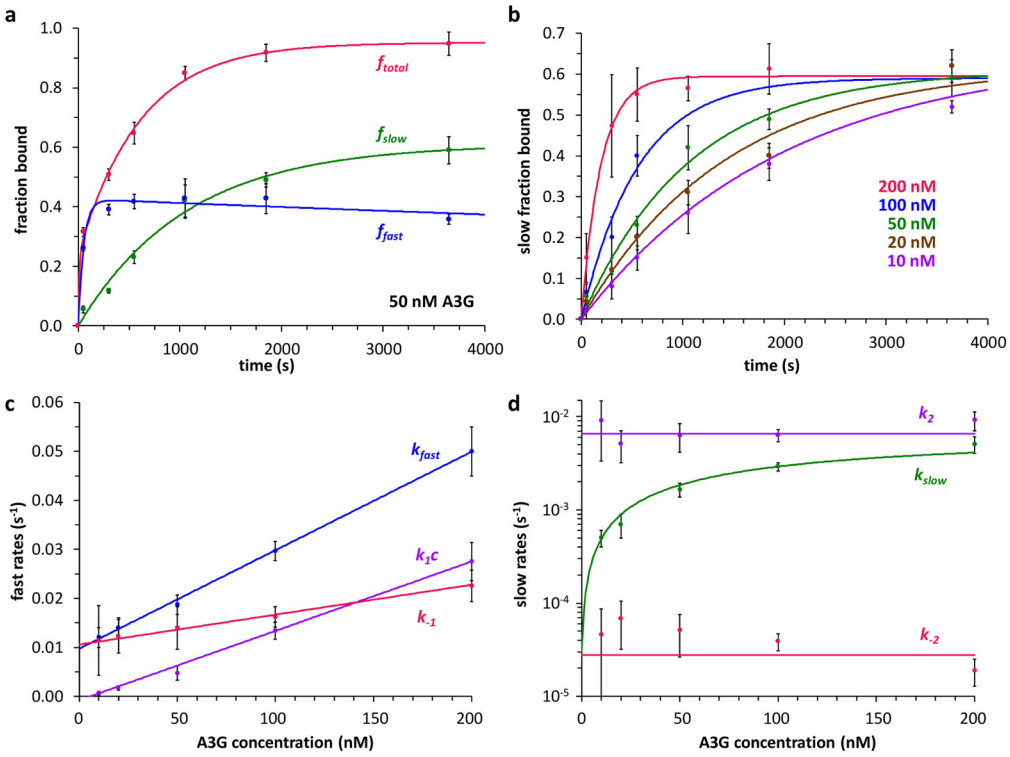

Figure 3.

Quantifying A3G binding reveals association and dissociation rates for fast and slow binding modes. (**a**) Total binding at 50 nM A3G ($f_{total,}$ red) separated into a fast fraction (f_{fast}, blue) and slow fraction (f_{slow}, green), as a function of ssDNA-A3G incubation time. Fits to the binding model (solid lines, Supplementary Eqs. S9–S11) yield observed rates k_{fast} and k_{slow}. (**b**) Slow fraction bound as a function of time for five A3G concentrations. Solid lines are fits to Supplementary Eq. S10. Error bars (panels **a, b**) are standard error (N≥3) for 50–200 nM A3G and propagated error for 10–20 nM A3G. (**c**) Fast rates (k_{fast}, blue data points) obtained from fits to the binding model (shown in panel **a** for 50 nM A3G). The linear fit (solid blue line, Supplementary Eq. S13) yields k_1 and k_{-1}. k_1c (purple data points) and k_{-1} (red data points) were also calculated from the binding model. Linear fits (solid lines, Supplementary Eqs. S15 and S17) yield consistent values of k_1 and k_{-1}. (**d**) Slow rates (k_{slow}, green data points) from fits to the binding model (panel **b**). Fits to Supplementary Eq. S21 (solid green line, see Supplementary Fig. 2, panel **b**) yield k_2 and k_{-2}. Separate calculations of k_2 (purple) and k_{-2} (red) from the binding model (Supplementary Eqs. S24 and S25) are also shown.

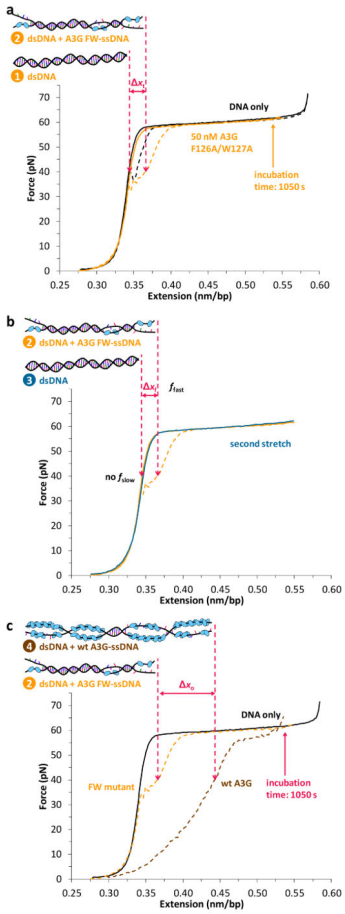

Figure 4.

Oligomerization-defective mutant F126A/W127A (FW) demonstrates that the slow kinetics observed for wild type A3G is due to oligomerization. (**a**) In the absence of protein (black), a single DNA molecule reanneals immediately upon release, exhibiting minimal hysteresis between extension (solid) and release (dashed). In the presence of 50 nM F126A/W127A A3G (orange), the stretch curve (solid) follows the dsDNA-only curve, indicating no measurable A3G FW binding to dsDNA (drawing 1). Pausing at fixed DNA extension after the melting transition to incubate the ssDNA with the protein results in ssDNA binding (drawing 2), indicated by the corresponding increase in length Δx_t measured during DNA release at a given force (shown for 40 pN). (**b**) The subsequent stretch (dark blue) follows the initial stretch curve (solid orange), indicating that all the mutant A3G bound during incubation dissociates rapidly (drawing 3), resulting in a decrease in length Δx_f. (**c**) Wild type A3G (drawing 4) exhibits a greater change in length Δx_o relative to the FW mutant (drawing 2) at 1050 s incubation due to oligomerization on ssDNA.

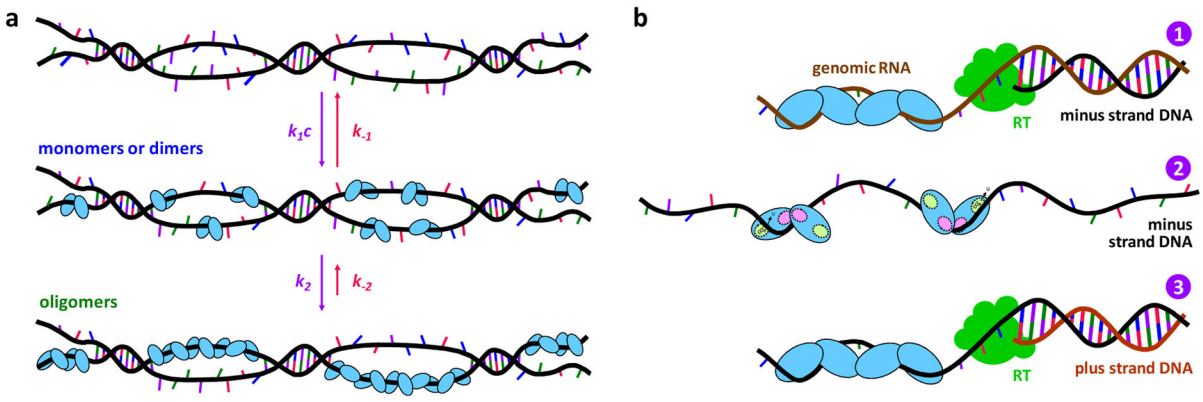

Figure 5.

Models for A3G oligomerization (A) *in vitro* and (B) *in virio*. (**a**) Initially monomers or dimers bind ssDNA with on rate k_1c and off rate k_{-1}. These forward and backward rates are on similar timescales ($1/k_1c$ = 33 ± 1 s at 200 nM A3G, and $1/k_{-1}$ = 85 ± 5 s), so fast binding reaches equilibrium before the monomers or dimers convert to oligomers ($1/k_2$ = 149 ± 13 s) on ssDNA. Oligomer dissociation is significantly slower ($1/k_{-2}$ = 10 ± 2 h) *in vitro*. (**b**) Inside the virus, A3G oligomerizes on the RNA genome, blocking minus-strand DNA synthesis by RT (panel 1). Once the oligomer dissociates, the monomers or dimers released bind ssDNA within a second, allowing rapid enzymatic activity (panel 2) until A3G oligomerizes on the ssDNA template in 150 s and blocks plus strand synthesis (panel 3).